Year 2 Final Report (Draft):

NOAA Joint Hurricane Testbed

Eastern Pacific Ocean Heat Content Estimates For SHIPS Forecasts*

Prepared by:

Lynn K. Shay and Jodi K.Brewster

Division of Meteorology and Physical Oceanography

4600 Rickenbacker Causeway

Miami, FL 33149

Phone: 305. 421.4075: Cell: 305.205.0305: Fax: 305. 421.4696

Email: nshay@rsmas.miami.edu

**Internet: D*aily EPAC estimates using the approach described herein can be found at: http://isotherm.rsmas.miami.edu/heat on our experimental web page and is running on TPC machines this year.

1. Introduction and Background:

Recent improvements to Statistical Hurricane Intensity Prediction Scheme (SHIPS) have shown that OHC parameter have reduced intensity forecast errors in the Atlantic Ocean Basin (DeMaria *et al.* 2005, Mainelli *et al.*, 2007). These studies have shown that the a seasonal Oceanic Heat Content climatology reduced forecast errors in intensity by an average of 2% when averaged over all storms between 1995 and 2003 compared to less than 1% from an annual analysis. If only the western part of the basin is used (60 to 100^{o}W), intensity errors are reduced from 3 to 6% when averaged over all storms. During the passage of hurricane Ivan in 2004, SHIPS with seasonal OHC showed as much as a 22% reduction in forecast intensity errors, which points to the importance of OHC in the warm pool of the Caribbean Sea and the Gulf of Mexico's Loop Current and warm core rings. Recent tests in the EPAC using the annual product have reduced errors in forecast intensity by about ~1%. Thus, the working hypothesis here is that intensity forecast errors will be reduced even further in SHIPS using a seasonal climatology to estimate daily OHC variability from satellites as described herein.

The Eastern Pacific Ocean basin (hereafter referred to as EPAC) is a region of significant upper oceanic variability given the warm pool and gradual shoaling of the oceanic thermocline from west to east, and the westward propagation of warm core rings forced either by low-level jets (Hurd 1929; Kessler 2003) or current instabilities (Hanson and Maul 1991) (Figure 1). A warm core ring moved southwestward at a 13 to 15 cm s^{-1} and dissipated within the Eastern Pacific Investigation of Climate (EPIC) domain in Oct 2001. In this warm pool regime, cyclogenesis often starts at ~10 to 14^{o}N and 90 to 100^{o}W, which is an area characterized by large sea surface temperature (SST) gradients and OHC variations that will impact hurricane intensity. Thermal gradients across the ocean mixed layer base are sharp starting about 40 m beneath the surface and the 20^{o}C isotherm separates the upper from the lower layer in a two-layer model. In Sept 2001 during hurricane Juliette's intensification to category 4, the SST cooling was less than 1^{o}C in a regime with strong vertical gradients (~20 cph: cycles per hour). Wind-driven ocean current shear tends to be insufficient to significantly cool the upper ocean through shear instability, but when Juliette moved into an area with weaker stratification (~10 cph); SST cooling was 4 to 5^{o}C. Entrainment mixing across the ocean mixed layer base due to ocean current shear did not lower the bulk Richardson number to below criticality. Hence, a larger fraction of OHC was available for Juliette through air-sea fluxes during the rapid intensification phase.

Thus, the overarching **goal** of this applied research effort was aimed at providing an OHC seasonal climatology for hurricane intensity forecasts from SHIPS. Specific objectives of this applied research project are*:*

1) *Develop and evaluate monthly OHC climatology with observed oceanic thermal and salinity structure data, surface height anomaly (SHA) and sea surface temperature (SST) fields starting in 1995; and,*
2) *Evaluate the performance of SHIPS with OHC for the EPAC using SHAs and SSTs to issue forecasts at TPC and CPHC.*

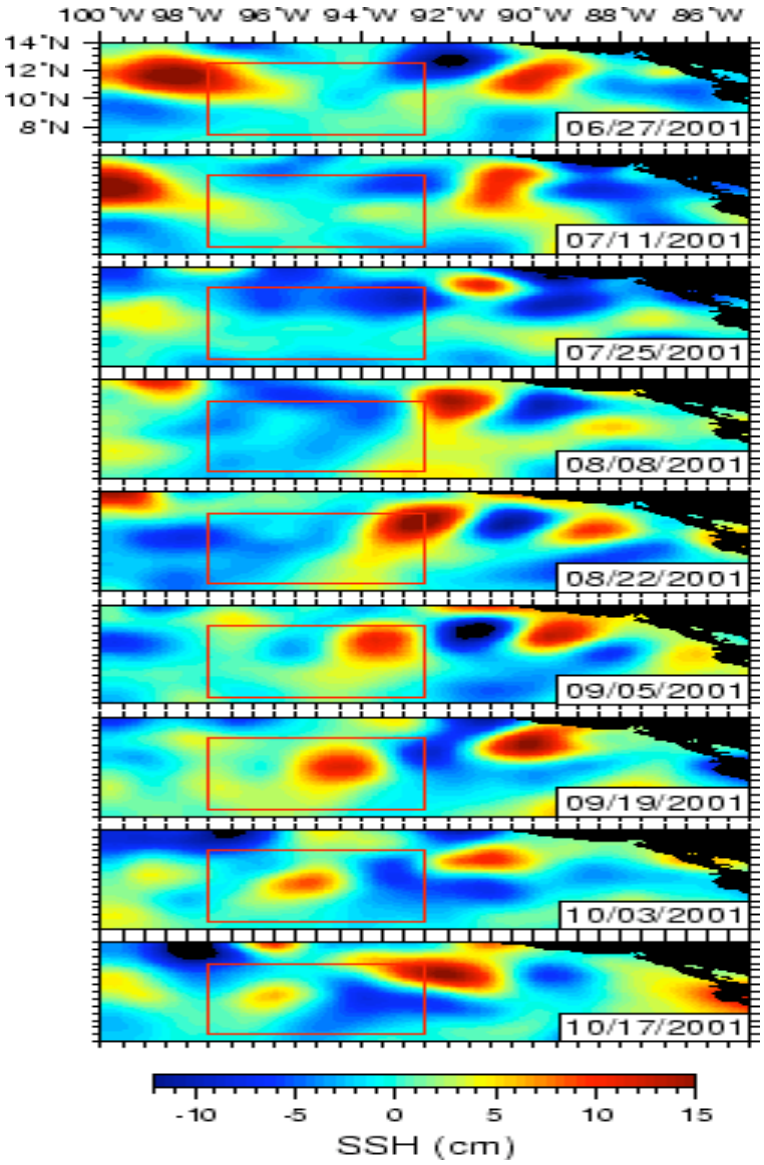

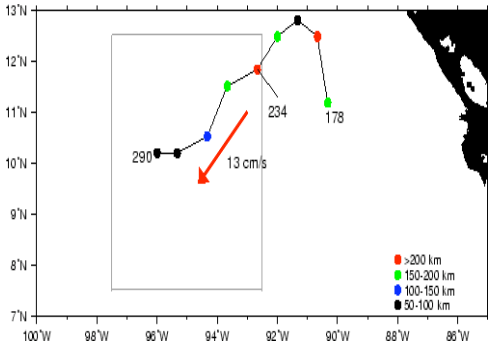

Figure 1: Sequential Sea Surface Height Anomaly (SHA: cm) in the EPAC relative to the EPIC domain in summer 2001 (left panel), and the pathway of the warm eddy feature (right panel) with the approximate diameter of the warm feature based on the 7 cm SHA contour. Merged SSH data is from the AVISO altimetry product.

Here, the 20ºC isotherm depth will be used as the level for a two-layer model to estimate reduced gravities (i.e. density differences between the upper and lower ocean layers). Satellite and *in situ* data will be used to assess the relationship between the 26ºC and 20ºC isotherm depths. Several *in situ* data sets are available to evaluate isotherm depths and OHC inferred from satellite remote sensing and a climatology in the EPAC.

To achieve these objectives, the research effort has primarily focused on processing data and synthesizing data sets in building a realistic climatology evaluated by making detailed comparisons to these data sets. The approach includes satellite radar altimeter data, Sea Surface Temperatures (SST), Tropical Atmosphere Ocean (TAO) mooring data spanning the Pacific Ocean equatorial wave guide, EPIC data, and assessing climatologies such as the US Navy's Generalized Digital Environmental Model (GDEM) to build a carefully evaluated ocean heat

content seasonal climatology for EPAC and SHIPS forecasting. The approach follows from previous work such as Shay *et al*. (2000) and Mainelli *et al*. (2007).

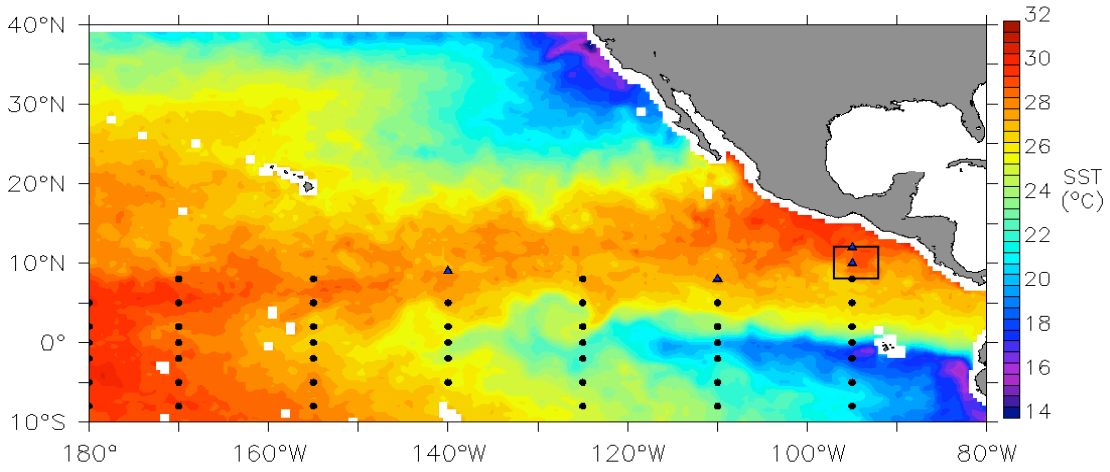

Figure 2: SST image from TRMM microwave imager (TMI: ºC) relative to the TAO moorings (black circles) and the EPIC warm pool domain (box). Triangles represent mooring data where comparisons have been done as part of this JHT sponsored study. (TMI data are courtesy of Dr. C. Gentemann of Remote Sensing Systems).

2. Data Resources

In this section, data resources are described for developing a seasonal ocean heat content climatology for the EPAC. As shown in Figure 2, TAO moorings relative to the EPIC domain are superposed on a Sept 2001 SST image. These mooring were originally deployed as part of the Tropical Ocean Global Atmosphere Program in the 90's and were enhanced at 95ºW during EPIC as noted in Cronin *et al*. (2002).

2.1 Radar Altimetry:

TOPEX/ Poseidon (T/P) and Jason-1 altimeter measures the sea level every 9.9 days along repeat ground-track spaced 3º longitudinally at the Equator. ERS-2 mission and U. S. Navy Geosat Follow-On-Missions (GFO) have repeat tracks of 35 and 17 days, respectively. More recently, Envisat data has been added since ERS-2 is no longer providing data. The availability of such measurements is shown in Figure 3 for several satellites that carry radar altimetry sensors. For example the NASA TOPEX began in 1992 (Cheney *et al*. 1994) followed by Jason-1 in 2000 as the follow on to TOPEX. As noted in Figure 1, altimetry data is useful in tracking oceanic mesoscale features. Weekly SHA fields allow one to track both warm and cold core eddies from Aug through Oct 2001 using this AVISO product during the EPIC field program. The ring pathway, tracked over a three-month period shown in successive images, suggests that the warm feature moved at 13 to 15 cm s^{-1} towards the west southwest as its diameter decreased during the decay process based on the SHA of 6 cm. Leben (2005) developed a comprehensive set of metrics to examine the kinematics and dynamics of Loop Current and Warm Core Ring shedding events using radar altimetry measurements in the Gulf of Mexico.

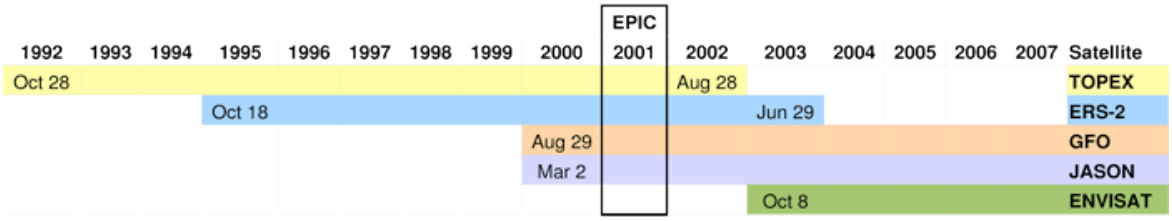

Figure 3: A timeline of start and end dates of various space-based radar altimeters in space acquiring measurements of the SHA fields used in this study.

In the forthcoming analysis, we restrict ourselves to periods when there are at least two sets of radar altimeter data available. These data are objectively mapped to a 0.5° grid using the approach of Mariano and Brown (1992). The oceanic analysis decomposes a scalar observation into three components using parameters derived from the hurricane Gilbert data set (Shay *et al.* 1992). Based on this approach, the first part of this scalar field is the large scale or trend field. The second component is represented by the synoptic time scale or the field variability on the mesoscale. That is, the composite SHA field from the 10- and 17-days of altimeter tracks from the various platforms is considered synoptic in time as each day this field is updated with the latest tracks of data. The last component represents unresolved scales, ie. noise and errors. Each day, the final field estimates of the SHA data are a sum of the trend field and the objectively mapped deviation field in space (Mainelli *et al*. 2001). In this procedure, the mapping noise is significantly reduced by adding additional platforms. That is, two or three sets of altimeter data minimize the mapping error of the objectively mapped field. This analysis procedure allows the SHA data to accurately depict (and track) mesoscale features as well as areas of strong horizontal thermal gradients each day when the latest data arrives.

Although the 10- and 17-d repeat cycles utilized in the OHC estimates are long compared with the time scale of the tropical cyclone, they are reasonable compared to the time scales of variability in the upper ocean, such as the ocean eddies being analyzed. Moreover, this analysis system is designed to be updated daily to incorporate altimetry measurements from all sensors including Envisat, which will further improve the OHC estimates, particularly in areas where the signal to noise ratios are large.

2.2 EPIC data:

The Eastern Pacific Investigation of Climate (EPIC) field program was conducted in and over the warm pool and along the 95°W transect to improve our understanding of these upper ocean processes and determine their relationship to the atmosphere boundary layer. During the field program (Weller *et al*., 1999; Raymond *et al.,* 2004), oceanic current, temperature and salinity measurements from Airborne eXpendable Current Profilers (AXCP), Airborne eXpendable Conductivity Temperature and Depth (AXCTD) profilers and Airborne eXpendable Bathythermographs (AXBT) were acquired from NOAA WP-3D and NCAR WC-130 research aircraft (see Table 1). Profilers were deployed from 19 research flights encompassing the warm pool and ITCZ and along the 95°W equatorial transects in Sept and Oct 2001. Oceanic profilers

were complemented with flight-level winds and atmospheric profiler data from GPS sondes. Flight tracks were located on each side of the *R/V Brown* and *R/V New Horizon* centered on the 10°N TAO mooring (Wijesekera *et al.* 2005).

NOAA WP-3D Missions						NCAR WC-130 Missions					
Date	Type	GPS	CP	CTD	BT	Date	Type	GPS	CP	CTD	BT
9/13	Gr	23/0	28/4	19/0	0	9/12	Test	0	1/1	2/0	8/0
9/16	Gr	31/7	28/5	20/8	0	9/14	95W	14/1	6/3	5/0	13/7
9/20	Gr	26/3	26/8	19/2	0	9/19	95W	13/0	5/2	7/1	12/2
9/21	JI	11/1	0	0	10/1	9/23	95W	14/2	6/2	6/1	12/2
9/28	Gr	8/0	4/0	3/1	0	9/25	95W	14/1	6/0	7/0	12/0
10/3	Gr	16/2	26/4	20/1	1/1	10/2	95W	13/0	5/0	6/2	13/0
10/5	Gr	17/4	27/5	19/2	0	10/3	SST	0	0	0	15/4
10/6	Gr	20/3	0	0	45/6	10/5	SST	0	0	0	15/2
10/7	Gr	19/1	27/1	29/5	0	10/9	95W	15/0	5/1	9/2	18/3
						10/10	95W	14/0	8/1	9/1	20/16
						Tot:	19	243/26	208/37	170/44	194/32

Table 1: Summary of EPIC research flights from the NOAA WP-3D and NCAR-WC-130 where **Gr** is grid flight, **95°W** is transect flight, **JI** is a Juliette Invest flight, and **SST** is a cold tongue flight, **CP** is a current profiler, **CTD** is a temperature and salinity profiler and **BT** is temperature profiler only. Failures are to the right of the slash under each category.

Objectively mapping the thermal structure from the grid measurements revealed the warm eddy structure (Figure 4) is consistent with SHA measurements shown in Figure 1. OHC values estimated from these snapshots range between 50 to 55 kJ cm^{-2} compared to more than 100 kJ cm^{-2} in the Loop Current. The depth of the 26°C isotherm depth exceeds 45 m in the warm ring, and decreases to 20 m outside of it. As the warm ring propagated southwestward in Oct, the isotherm depth decreased to about 15 m in the approximate region of the Costa Rica Dome along the eastern portion of the domain (Hofmann *et al.* 1981). This spatial variability in the warm rings has a pronounced impact on the OHC distributions.

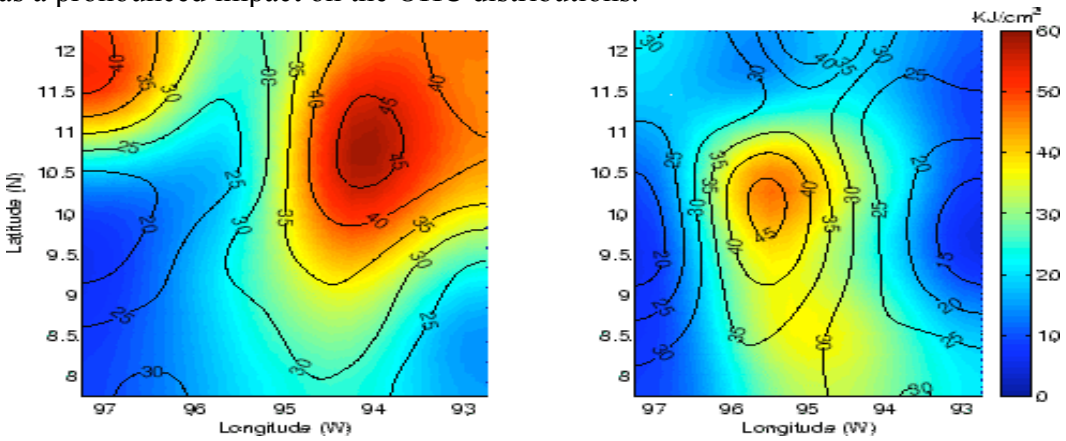

Figure 4: Averaged OHC (kJ cm^{-2}) from *in situ* thermal profiles during EPIC in Sept (left panel) and Oct (right panel) based on AXCPs and AXCTDs temperature structure from aircraft.

2.3 TAO Mooring Data:

Time series of thermal structure measurements from NOAA TAO moorings in the EPAC deployed as part of the long-term monitoring by Pacific Marine Environmental Laboratory have been processed (Cronin *et al*. 2002). EPIC-enhanced TAO moorings acquired measurements of temperature at 1, 5, 10, 20, 40, 60, 80, 100, 120, 140, 180, 300 and 500 m, and salinity at 1, 5, 10, 20, 40, 80 and 120 m at 8, 10 and 12ºN, 95ºW ITCZ and warm pool mooring sites (Cronin *et al*. 2002). TAO temperature structure data from moorings at 95ºW, 110ºW and 140ºW will be used here in assessing the OHC climatology based on satellite sensing. Over several years of measurements, TAO time series from May through October will be used to evaluate remotely sensed OHC values.

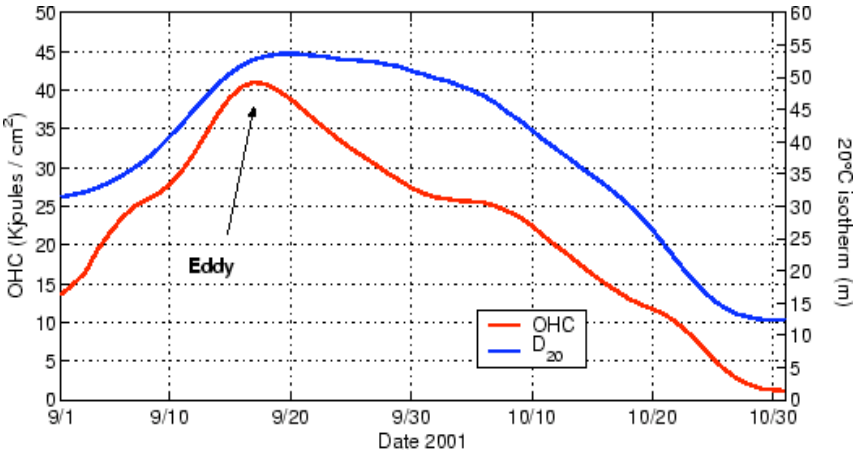

Figure 5: OHC (kJ cm^{-2}) and the 20ºC isotherm depth (m) determined from the TAO mooring at 10ºN95ºW during Sept and Oct of 2001 during the EPIC field program**.**

As shown in Figure 5, an example of a depressed thermocline (i.e. 20ºC isotherm depth) occurs during the passage of a warm core ring at 10ºN and 95ºW. That is the warm eddy has warmer water at depth which causes a positive SHA detected by radar altimeters. At this position, the OHC values exceeded 40 kJ cm^{-2} as the eddy began to spin down and weaken, consistent with Figures 1 and 4.

3. Approach:

Based on recent analysis, the approach in the Atlantic Ocean basin of Shay *et al*. (2000) and Mainelli *et al*. 2007 has been revised for application in the EPAC. The rational is that the stratification is much stronger in the EPAC where the stratification or buoyancy frequency (i.e. the vertical derivative of the density structure) has a maximum (N_{max}) value of 24 cycles per hour (cph) compared to values of 6 to 12 cph in the Atlantic basin (Figure 6 right panel). The vertical salinity changes (not shown) at the base of the oceanic mixed layer (h) contribute to these density changes. However, upper ocean salinities in the EPAC tend to be less than in the Gulf of Mexico due to the ITCZ where excess rainfall reduces the mixed layer salinities compared to the Gulf of Mexico. The shoaling thermocline from west to east sets this large value of N, which is a close proxy to the 26ºC isotherm depth needed for the OHC estimations.

3.1 Empirical Model:

As the algorithm represents the area underneath the curve (Fig. 6 gray area), the OHC in the oceanic mixed layer (h) relative to the remotely sensed SST from TMI is proportional to the product *[(SST-26°C) x h]* plus the contribution underneath the layer from h to the depth of the 26ºC isotherm using the SST given by *0.5 [H_{26} -h][SST-26°C]*. The total OHC is the addition of the mixed layer contribution plus the contribution from the mixed layer depth to the isotherm depth. There are a few caveats associated with this empirical model:

1. The seasonal climatological mixed layer has its own density that sits on top of a two-layer fluid; and,

2. The ocean mixed layer depth is time invariant since we do not have surface heat fluxes, wind stress or current shear at the base of the oceanic mixed layer to determine its' evolution.

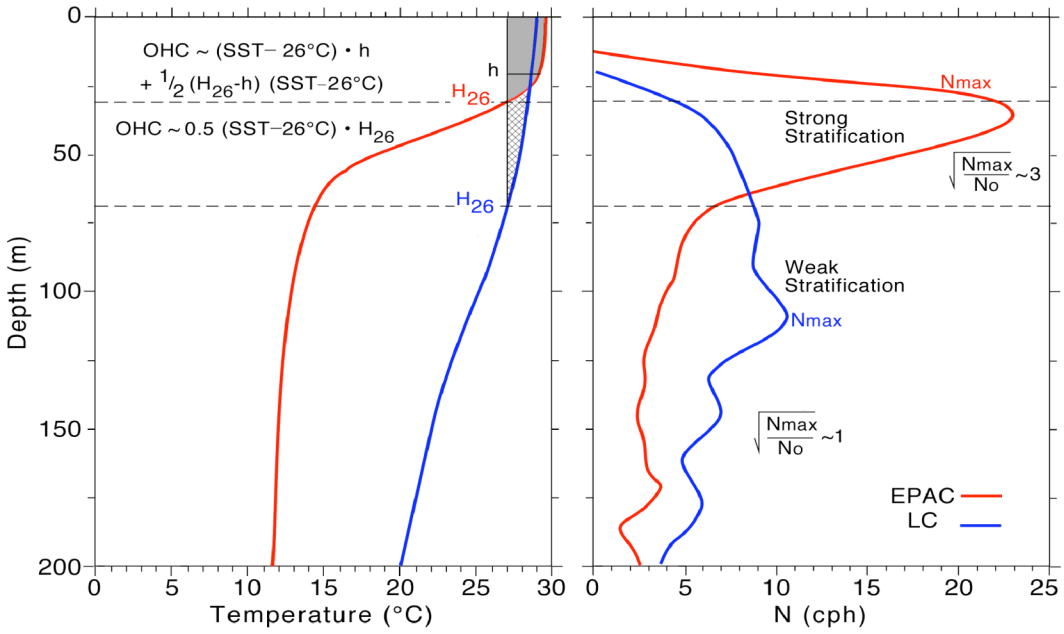

Figure 6: Cartoon of the revised empirical approach for the EPAC based on two AXCTD profiles shown in red curves (shaded area) compared to the approach used in the Atlantic Ocean basin shown in blue curves (hatched area) in the temperature (left panel:ºC) and the corresponding N profiles (right panel: cph) that reflects strong stratification (EPAC-red) and weak stratification (Loop Current-blue), h is the ocean mixed layer depth and H_{26} represents the 26ºC isotherm depth. Notice the ratios of the maximum buoyancy frequency (N_{max}) to the reference buoyancy frequency (N_o). Notice the square root of this ratio is a factor of two to three times greater in the EPAC than in the LC.

Variations in the SHA field have maximum impact in the seasonal thermocline (i.e. 20ºC isotherm depth) and have a minimal impact on h. This approach must be equally tested in the

Atlantic Ocean basin to assess whether there is an improvement in the OHC estimates. However, previous comparisons based on seasonal climatology have indicated good agreement between satellite-inferred and observed OHC estimates in the Gulf of Mexico given its weaker thermal structure and vertical density changes compared to that observed in the EPAC (Shay 2007).

3.2 U.S. Navy Generalized Digital Environmental Model

Central to this vertical structure issue is its representation in climatology and in situ data. In comparing the two climatologies (**V2.1** and **V3 GDEM**) on monthly and seasonal time scales, an important issue is determining the oceanic mixed layer depth (Teague *et al.* 1990). For example, the ocean mixed layer (h) by definition is well mixed in properties such as temperature and salinity. Close inspection of the salinity profiles for September reveal significant differences between salinity in the upper 10 to 15 m of the water column (not shown). That is, the salinity structure in **V2.1** reveals no constant salinity in this near-surface layer, by contrast, the salinity is relatively constant in the layer from 15 m to the surface. While these vertical salinity changes affect the density structure, the thermal structure dominates the density in the upper ocean which seems to be more realistic in **GDEM V2.1** than **V3.0**. For example, the well-mixed ocean mixed

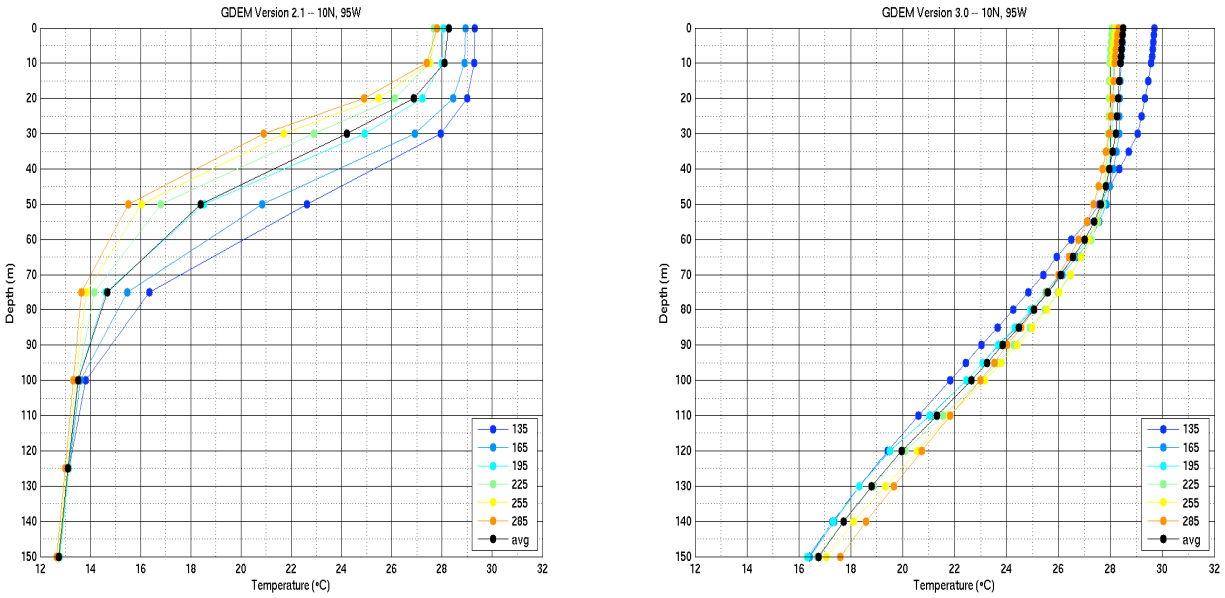

Figure 7: Monthly temperature profiles from GDEM **V2.1** (left panel) and **V3.0** (right panel) at 10°N and 95°W in the upper 150 m from May through October. Mean temperature profile is black line.

layer (in terms of temperature) depth decreases from a maximum in May of 30 to 40 m to a minimum of about 15 m in October. Such thermal structure behavior is generally more in line with observed thermal structure variations during from the EPIC CTD profiles. That is, this layer shallowing from the EPIC data suggests that the ocean mixed layer is about 20 to 25 m deep in the warm pool or about 5 to 10 m deeper than the September climatology. Of equal importance is the vertical temperature structure beneath the layer that is more in line with the CTD profile as

well in **GDEM V2.1**. However, over the season from May to October at 10°N and 95°W, climatologies suggest a shallowing of the surface mixed layer to about 10 m.

Accordingly, this approach will use an earlier version of GDEM climatology for this grant and the analysis contained herein. This is also the same version used for the Atlantic Ocean basin to ensure consistency between the two basins. Climatologically, the SSTs exceed 28°C in the EPAC as shown in Fig. 8a. The spatial variations in the surface mixed layer depth are shown in Figure 6b based on an average from May through October. Notice how the oceanic mixed layer depth shoals towards the east where mean values range between 15 to 20 m as compared to h of more than 80 m west of 120°W. These spatial changes in h are now reflected in the approach.

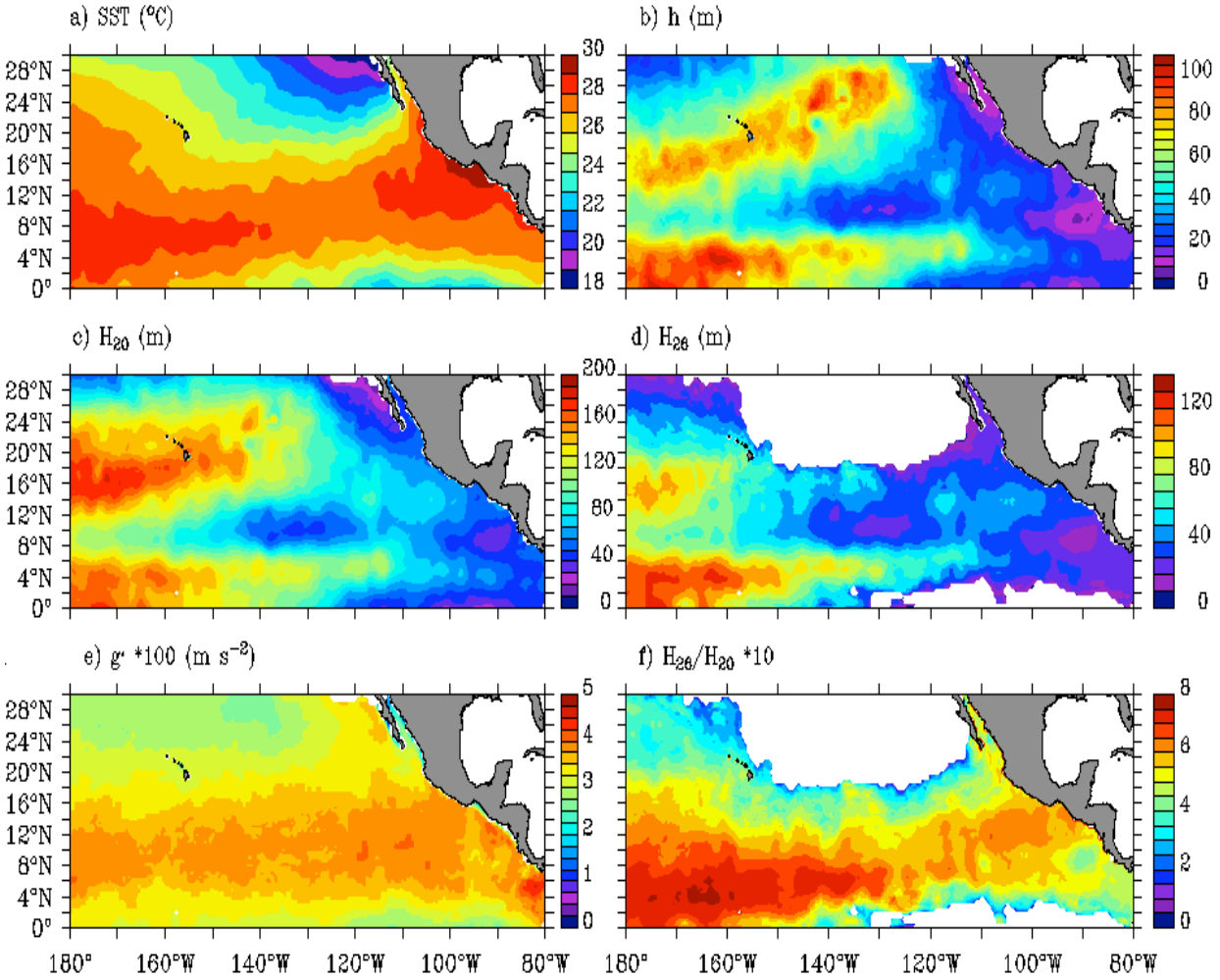

Figure 8: Hurricane seasonal climatology values for a) SST (°C), b) h (m), c) H_{20} (m) , d) H_{26} (m), e) g' (x 10^2 m s^{-2}) and f) $H_{26}\,H_{20}^{-1}$ (x 10) from **GDEM V2.1** for use with the empirical approach outlined in Figure 6.

As shown in Figure 8c,d, the seasonal mean depths of the 20° C and 26°C isotherms are based on an average over a hurricane season using GDEM profiles at 0.5° resolution. Notice the general shoaling of the isotherm depths from west to east that forces tighter vertical gradients in the

warm pool's upper ocean thermal structure (and shallower ocean mixed layer depths). Generally, the 20ºC isotherm depths range from 30 to 50 m compared to more than 100 m west of 140ºW. The corresponding 26ºC mean isotherm depth ranges between 15 to 25 m in the warm pool (12ºN, 95ºW) and north of 20ºN, the 26ºC isotherm shoals to the surface. This surface shoaling, known as ventilating of the 26ºC isotherm, implies that once a TC reaches that area, they will begin to lose their oceanic heat source and begin to weaken. A second aspect of this area is that the buoyancy frequencies at the base of the ocean mixed layer exceed 20 cph as suggested in Figure 6.

As per the model, reduced gravity (g') distribution (density difference between upper and lower layer multiplied by the acceleration of gravity) and the ratio between the 26ºC and 20ºC isotherm depths are shown in Fig. 8e,f. East of 120ºW, reduced gravities are about 5 x 10^{-2} m s^{-2}, which is indicative of the strong stratification of the EPAC. West of this longitude, g' decreases to about 3.5 x 10^{-2} m s^{-2} whereas towards the northern part of the domain, reduced gravities decrease to about 2 x 10^{-2} m s^{-2}. For example, in the area of hurricane Norbert experiment (1984), the observed buoyancy frequency was 11 to 12 cycles per hour (cph) compared to more than 20 cph in the warm pool (Shay *et al.* 1989). Such spatial variations have a pronounced impact on cooling and the generation of a cold wake or trail left behind by the hurricane. In general, the strong stratification in the warm pool often precludes a strong internal wave wake left behind by hurricanes. During hurricane Juliette in 2001 (not shown), the cold wake of SSTs exceeding 4ºC only began towards the north and west of the warm pool (Shay and Jacob 2006).

3.3 Ocean Heat Content Estimation:

As shown in Figure 9, the OHC is estimated using **GDEM V2.1** climatology from Figure 6 using the surface height anomaly (SHA) and TMI-derived Sea-Surface Temperature (SST) fields for mid-September 2001 to coincide with EPIC. The approach uses SHA from TOPEX, GFO, and ERS-2 altimetry data (not the blended AVISO in Figure 1) where repeat tracks are 9.9, 17 and 35 days, respectively. These fields are blended and objectively analyzed to a 0.5º grid from the coast to 180ºW and from the equator to 30ºN and are then combined to estimate isotherm depths and OHC. As shown in Fig. 9a, the warm SSTs exceeded 27.5ºC north of the equatorial cold tongue and extended longitudinally from the coast to 180ºW. Cooler SSTs are observed north of 20ºN, and decrease to below 26ºC at about 24ºN. The mean 20ºC isotherm depths suggest a general shoaling from west to east to a relative minimum of about 40 m in the EPIC domain. Notice the general shape of this minimum that apparently was affected by a warmer feature between the two cold cells (Fig. 9b). This may be a manifestation of the Costa Rica Dome, which is a semi-permanent feature of the EPAC due to the cyclonic mean wind stress curl (Hofmann *et al.* 1981). The 26ºC isotherm depths also show a similar pattern except that the relative minimum is about 20 to 25 m. Finally, the resultant OHC distribution shows values of ~50 kJ cm^{-2} at ~14ºN and 95ºW. As suggested by Figure 4, a key issue is the OHC distribution within the EPIC domain should have a similar value but is actually 12 kJ cm^{-2} less than observed.

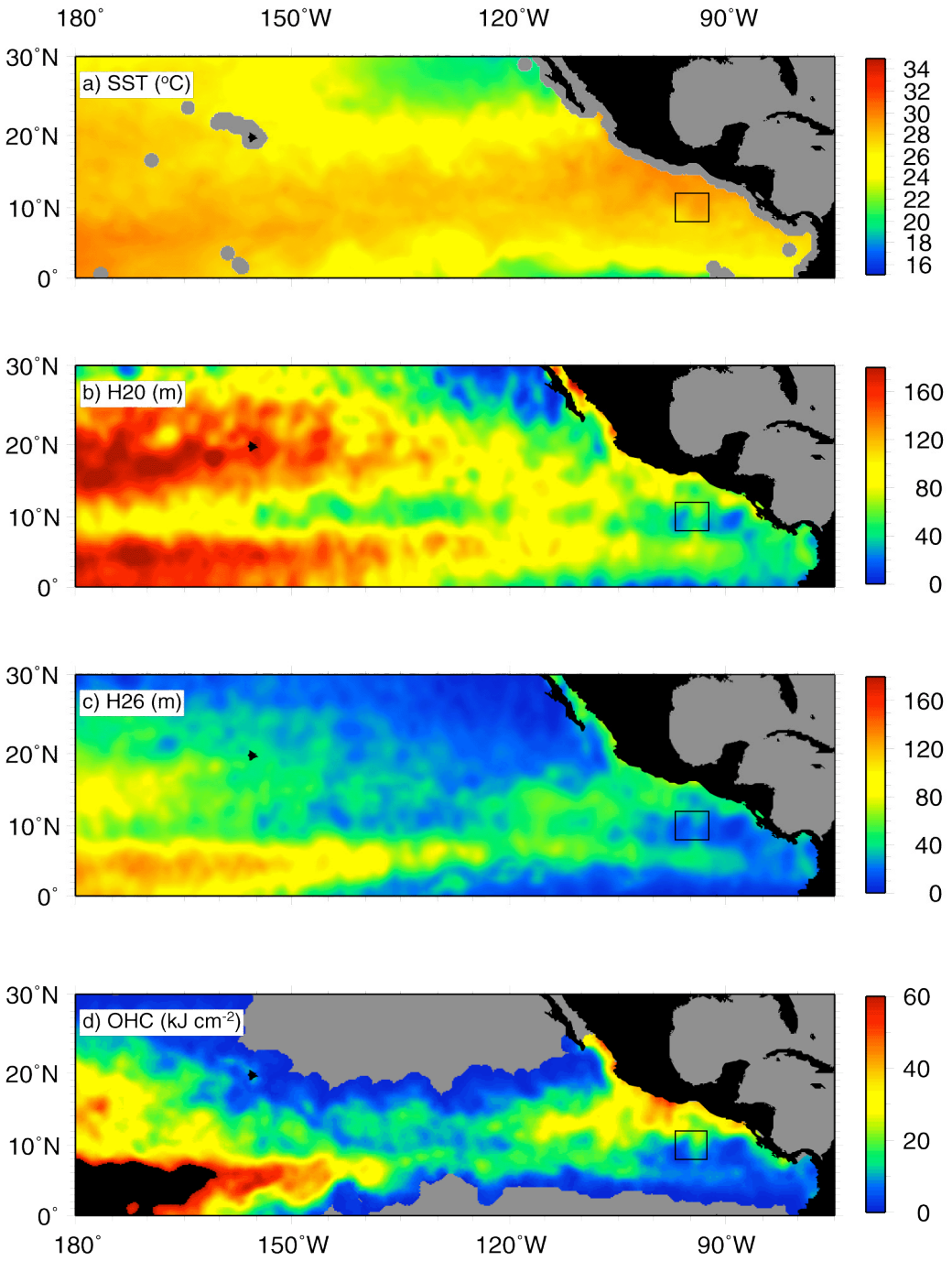

Figure 9: a) TMI-derived SST (°C) , b) H_{20} (m), c) H_{26} (m), and d) OHC (kJ cm^{-2}) in the EPAC for 15 Sept 2001 during the EPIC field program as depicted by the black box centered at 10°N and 95°W.

3.4 Sea Surface Temperatures:

The surface boundary condition is central to these satellite retrievals as suggested in Figure 6. As shown in Figure 10, SSTs from Reynolds, TMI and TAO mooring data are compared using regression techniques. For example, TAO mooring derived data suggest warmer SSTs than those derived from Reynolds analysis (slope of the least squares fit is 0.63) with RMS differences of about 0.6ºC. The better comparison is between TAO and TMI data where the RMS difference is

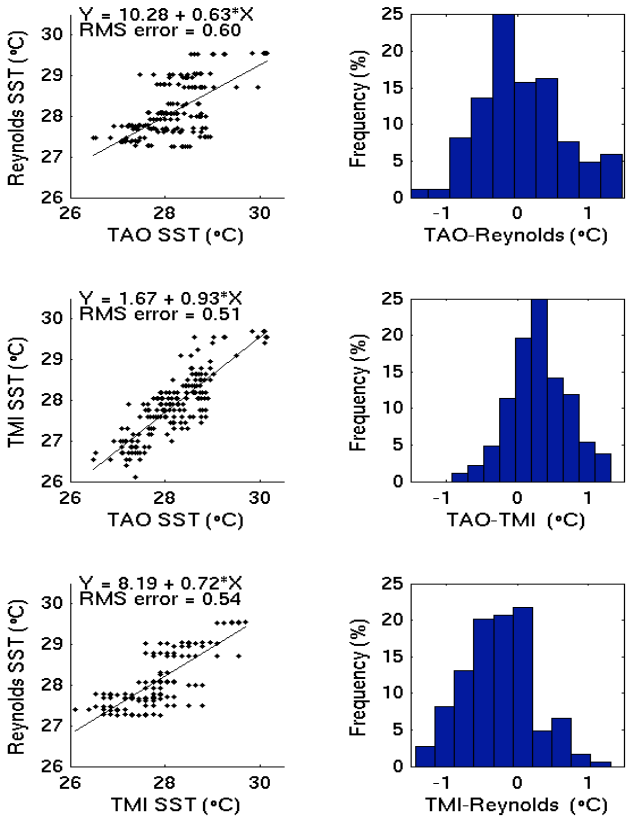

Figure 10: Regression analysis (left panel) and histograms of differences in SST (ºC) measurements (right panel) between TMI, Reynolds, and the TAO 1-m mooring data at 10ºN, 95ºW from May through Oct 2001. The regression line (including the linear equation) and RMS differences are given for each analysis.

0.5ºC. Note that in this comparison, the slope of the regression curve is 0.93-indicative of a better fit with a bias of 1.7ºC. Finally, the Reynolds analysis is compared to the TMI SSTs. The RMS differences are 0.54ºC and the slope of the regression curve is 0.71 with a bias of 0.2. In general, Reynolds-derived SSTs tend to be higher than the TMI SST. Note the TMI data are corrected for diunal cycling (Gentemann 2007). Notwithstanding, the point is that not all SST products are equal, and when it represents the surface boundary condition, care must be afforded to the most appropriate choice of the data stream for OHC estimation for input into SHIPS.

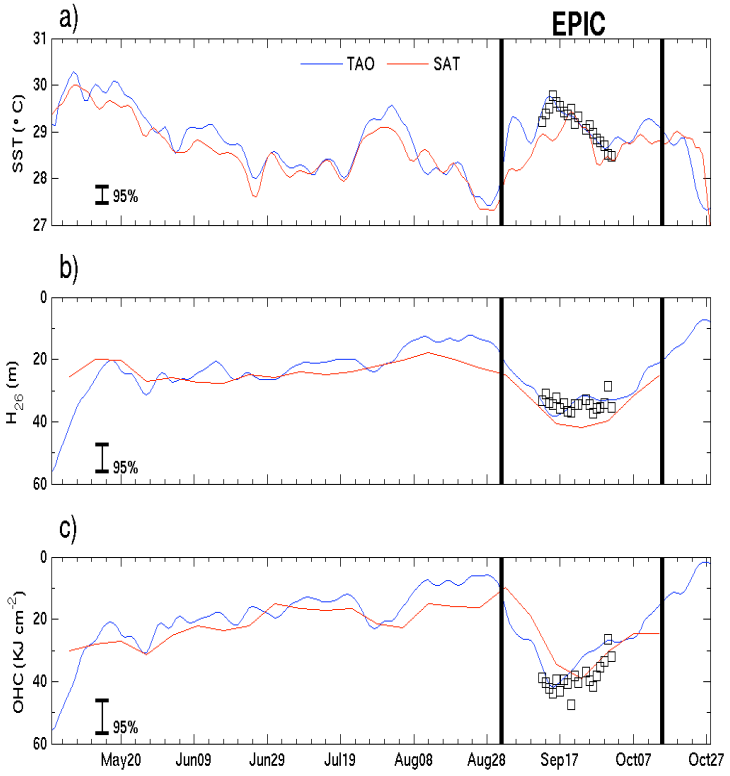

Figure 11: EPAC hurricane season comparisons in 2001 for a) SST (ºC) , b) H_{26} (m) and c) OHC (kJ cm^{-2}) from TAO mooring at 10ºN, 95ºW (blue), satellite-derived (red) based on GDEM V2.1, and CTD profiles (boxes) from the *R/V Ron Brown* acquired at the TAO mooring during EPIC experiment from 1 Sept to 15 Oct 2001. The 95% confidence interval is based on the *student-t test* for comparing two sets of mean quantities.

4. Observational Comparisons:

An important aspect of this applied research is to understand differences between directly observed values and those inferred from satellite remote sensing techniques (Figure 11). Observed SSTs, 26ºC isotherm depth and OHC values from the TAO mooring at 10ºN and 95ºW (as well as CTD profiles from *R/V Ron Brown)* are compared to satellite-derived fields based on the AVISO images in Figure 1 that use the TMI and the **GDEM V2.1** climatology. SSTs from 1-m depth on the TAO mooring are in good agreement with those from the satellite-derived SSTs over the time series. Here, the approximate 0.5ºC differences are attributed to the fact that the TMI sensor sees only skin temperature whereas the TAO data represent a more bulk measurement in the upper part of the surface mixed layer. However, the depth of the 20ºC isotherm suggests about a 15 m difference between observed and satellite inferred. The TAO mooring data suggests shallower isotherm 20ºC isotherm depth compared to the satellite-derived isotherm depth. Since the TAO mooring data are acquired at discrete depths of 20, 40 and 60 m, the comparison to the CTD profiles to the *R/V Brown* indicate that the derived depth from the TAO moorings may actually be a bit deeper. As shown in Fig. 11b, however, the satellite inferred 26ºC isotherm depth shows a much higher correlation to this observed isotherm depth. Note that as the eddy passes the mooring, in mid-September, both isotherm depths reflect a deeper warmer layer. The corresponding OHC (Fig. 11c), derived from the satellite data, range in values of 20 to 30 kJ cm^{-2} prior to eddy passage. As the eddy passes over the mooring, it increases to about 40 kJ cm^{-2} where the TAO mooring suggests a larger value of 43 kJ cm^{-2} compared to 38 kJ cm^{-2}.

	10ºN,95ºW			12ºN,95ºW			8ºN,110ºW			9ºN,140ºW		
	Bias	Slope	RMS	Bias	Slope	RMS	Bias	Slope	RMS	Bias	Slope	RMS
H20	-2.8	0.9	13.6	17.2	0.7	13.2	29.	0.8	15.5	8.7	0.8	10.9
H26	-0.5	0.8	8.2	12.6	0.6	8.9	18.	0.5	11.5	18.8	0.4	12.2
OHC	-0.5	0.8	7.9	11.6	0.7	10.3	-0.7	0.8	9.8	0.6	0.8	8.9

Table 2: Bias, slope and RMS differences of the 20ºC, 26ºC isotherm depths (m) and OHC (KJ cm^{-2}) values from 2000-2003 based on a linear interpolation of the thermal structure and the GDEM V2.1 climatology and TMI-derived SSTs and blended radar altimetry.

In addition to the 10ºN and 95ºW TAO moorings during EPIC, we have made comparisons at four TAO sites 10ºN, 95ºW, 12ºN, 95ºW, 8ºN, 110ºW and 9ºN, 140ºW to assess spatial variations in the satellite algorithm to reflect the Eastern Pacific Ocean variability and not just the warm pool from 2000 to 2003 (Table 2). The method of determine the isotherm depths is based on a linear interpolation in the vertical which will induce large biases (i.e. 110ºW). In fact, the corresponding slopes between TAO and satellite inferred lies between 0.4 and 0.6 for the 26ºC isotherm depth compared to results at 10ºN, 95ºW. As shown in Figure 12, the four-year comparisons for OHC is promising in that the RMS differences range from 8 to 10 KJ cm^{-2} at all four locations. The dynamic range of the OHC ranges from nearly zero to values as high as 80 KJ cm^{-2}. Thus values reflect about 10 to 15% differences assuming no errors in the TAO mooring data. These comparisons suggest that we will need to use a polynomial fit of the temperature structure in both the **V2.1** climatology and the TAO *in situ* data since linear interpolation may lead to an underestimate of the 26ºC isotherm depth and OHC. This is important given the strength of the vertical density gradients (primarily temperature) at the base of the oceanic mixed layer as per Figure 6 based on CTD profiles.

For the twelve years of data, 1995 to 2006, we will incorporate the polynomial or cubic spline approach in resolving the isotherm depths prior to estimating OHC from the climatology. We have assessed this with these four years of measurements in the climatology fields and found differences of about 8 to 10 m in the 20ºC isotherm and about 3 to 6 m in the 26ºC isotherm depth. This has an impact on the relative ratio of these isotherm depths (Figure 8f) and on estimating these depths from the altimeter data. We will be finishing these comparisons over the next few months and implementing a revised climatology. This approach is relatively easy to implement, but the time consuming part of this research effort is running the empirical approach on 12 years of data. These multiyear data series are required so that CIRA can train the SHIPS model for operational forecasting in the EPAC. We are addressing both of these questions prior to forwarding the seasonal hurricane climatology to TPC for use in SHIPS for next season (2008).

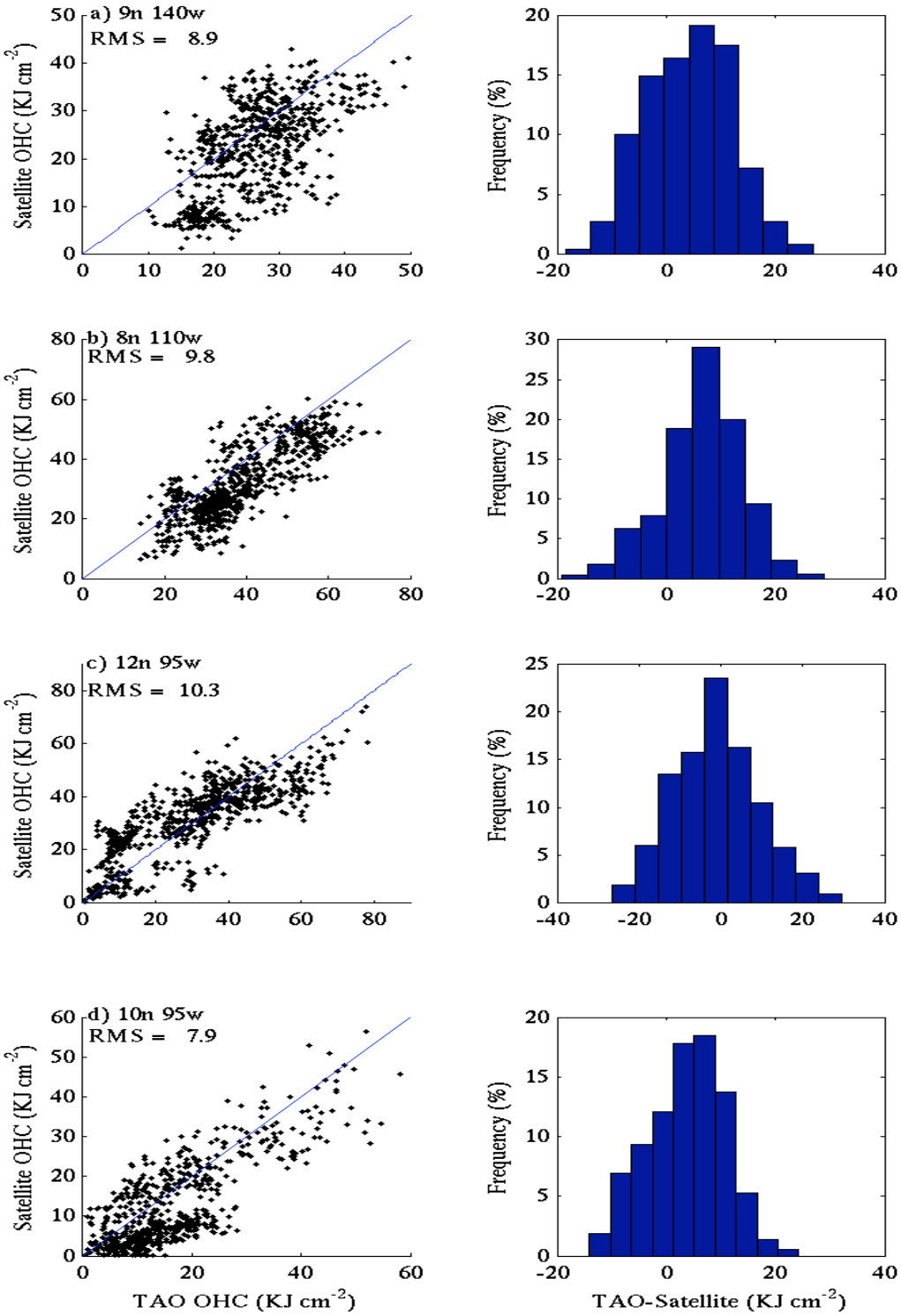

Figure 12: Scatter plot and histogram of differences between TAO (abscissa) and satellite-derived (ordinate) OHC (KJ cm^{-2}) for a) 8°N,140°W, b) 8°N,110°W, c) 12°N,95°W and d) 10°N,95°W from 2000 to 2004. Scatter plot shows the blue line for the perfect fit and the RMS differences based on the four years of data.

5. Summary and Concluding Remarks:

Over the two years of the grant, we have made substantial progress on developing a realistic climatology for the EPAC using GDEM V2.1 to be consistent with the Atlantic product used in SHIPS (DeMaria *et al*. 2005; Mainelli et al. 2007). Detailed evaluations of satellite-inferred values to observed profiles including estimates of the isotherm depths and OHC fields from the EPIC experiment and time series from the TAO moorings. These comparisons include data will also include TAO mooring locations (see Fig. 2) from 2000-2003. Following the approach above, the statistics will be improved with more data from differing platforms. It is a possibility that we may have to use a monthly climatology in the future.

We have generally met the schedule and the program objectives of this NOAA Joint Hurricane Testbed grant. In fact, daily estimates for the EPAC using the approach described herein can be found at: http://isotherm.rsmas.miami.edu/heat on our experimental web page and is running on TPC machines this year. The complete package will be delivered to TPC and CIRA in early 2008 that will include the climatology and empirical model and the 12-years of data in building a realistic climatology. While a four-year time series is adequate in understanding these differences, a 12-year time series will be more comprehensive and help us nail down the uncertainties in the measurements and the empirical model. Finally, we also anticipate writing a journal paper on this approach using the report as well as discussing the in situ data in the future.

Acknowledgments: National Science Foundation OCE-00-02459 and ATM-00-02363 supported the acquisition of the EPIC data anfd the NOAA Office of Global Programs provided the aircraft time. We are grateful for the efforts of the pilots, technicians, engineers and scientists at NOAA's Aircraft Operation Center (Dr. Jim McFadden, Captain Sean White). John Lyman provided the processed AVISO images. Dr. Chelle Gentemann from Remote Sensing Systems provided the processed TMI-SSTs.

6. References:

Cheney, R., L. Miller, R. Agreen, N. Doyle, and J. Lillibridge, 1994: TOPEX/Poseidon: the 2-cm solution. *J. Geophys. Res.*, **99**, 24,555-24,563.

Cronin, M. F., N. Bond, C. Fairall, J. Hare, M. J. McPhaden, and R. Weller, 2002: Enhanced oceanic and atmospheric monitoring underway in the Eastern Pacfic. *EOS,* **83(19)**, 210-211.

DeMaria, M. Mainelli M., L.K. Shay, J.A. Knaff, and J. Kaplan. 2005: Further improvements to the statistical hurricane intensity prediction scheme (SHIPS). *Wea. and Forecasting,* **20(4)**, 531-543.

Gentemann, C. L., 2007: Diurnal warming at the sea surface. PhD Dissertation, Division of Meteorology and Physical Oceanography, Rosenstiel School of Marine and Atmospheric Science, University of Miami, 169pp.

Hansen, D. V., and G. A. Maul, 1991: Anticyclonic current rings in the eastern tropical Pacific Ocean. *J. Geophys. Res.*, **96,** 6965-6979.

Hofmann, E., A. Busalacchi, and J. J. O'Brien, 1981: Wind generation of Costa Rica Dome, *Science*, **214**, 552-554

Hurd, W.E., 1929. Northers of the Gulf of Tehuantepec. *Mon. Wea. Rev*.,**57,** 192-194.

Kessler, W.S. 2002: Mean Three-Dimensional circulation in the Northeast Tropical Pacific. *J. Phys. Oceanogr.*, **32**, 2457-2471.

Leben, R. R., 2005: Altimeter derived Loop Current metrics. In Circulation in the Gulf of Mexico: observations and models, *Geophys. Monogr*., Vol **161,** Amer. Geophys. Union, 181-201.

Leipper, D., and D. Volgenau, 1972: Hurricane heat potential of the Gulf of Mexico. *J. Phys. Oceanogr*., **2**, 218-224.

Mainelli, M., L.K.Shay, S.D.Jacob, and P.G.Black, 2001: Operational heat potential estimates for hurricane intensity. 55th Interdepartmental Hurricane Conference, 5-9 March, 2001, Orlando, FL.

Mainelli, M., M. DeMaria, L. K. Shay and G. Goni. 2007: Application of oceanic heat content estimation to operational forecasting of recent category 5 hurricanes, *Wea and Forecast.* (***In Press)***

Raymond, D. J., S. K. Esbensen, C. Paulson, M. Gregg, C. Bretherton, W. A. Peterson, R. Cifelli, L. Shay, C. Ohlmann, and P. Zuidema, 2004: EPIC2001 and the coupled ocean-atmosphere system of the tropical East Pacific. *Bull. Amer. Met. Soc.*, **85(9),** 1341-1354.

Shay, L.K., Upper Ocean Structure: a Revisit of the Response to Strong Forcing Events. In*: Encyclopedia of Ocean Sciences*, ed. John Steele, S.A. Thorpe, Karl Turekian and R. A. Weller, Elsevier Press International, Oxford, UK (Submitted), 35 pp. ***(Accepted, Revised and Resubmitted)***

Shay, L. K. and S.D. Jacob. 2006: Relationship between oceanic energy fluxes and surface winds during tropical cyclone passage (Chapter 5). Atmosphere-Ocean Interactions II, *Advances in Fluid Mechanics*. Ed. W. Perrie, WIT Press, Southampton, UK. 115-142.

Shay, L.K., R.L. Elsberry and P.G. Black. 1989: Vertical structure of the ocean current response to a hurricane. *J. Phys. Oceanogr.*, **19**, 1249 - 1269.

Shay, L. K., G. J. Goni, and P. G. Black, 2000: Effect of a warm oceanic feature on hurricane Opal. *Mon. Wea. Rev*., **128**, 1366-1383.

Teague, W.J., M.J. Carron, and P.J. Hogan, 1990: A comparision between the Generalized Digital Environmental Model and Levitus climatologies. *J. Geophys. Res*., **95,** 7167-7183.

Weller, R. A., B. Albrecht, S. Esbensen, C. Eriksen, A. Kumar, R. Mechoso, D. Raymond, D. Rodgers, and D. Rudnick, 1999: *A science and implementation plan for EPIC: An Eastern Pacific Investigation of Climate Processes in the Coupled Ocean-Atmosphere System,* 105 pp.

Wijesekera, H., D. Rudnick, C. Paulson, S. D. Pierce, W. S. Pegau, J. Mickett and M. C. Gregg, 2005: Upper ocean heat and freshwater budgets in the eastern Pacific warm pool. *J. Geophys. Res.*, **110,** doi:10.1029/ 2004JC002511.